Journal of Structural Chemistry. Vol. 59, No. 6, pp. 1288-1298, 2018.

DFT STUDY OF THE STRUCTURAL AND ELECTRONIC PROPERTIES OF CONDUCTING OLIGO(*p*-FLUOROPHENYLTHIOPHENE)*

H. Nikoofard and A. H. Amin

A comprehensive theoretical study on the conducting oligomeric systems is carried out in view of their potential application in electrochemical charge storage. Density functional theory (DFT) calculations are carried out on a series of oligomers made up of 3-(*p*-fluorophenyl)-thiophene (FPT) to estimate the geometric and electronic structures, conjugated lengths, bandwidths, and energetic properties of polymeric systems. The calculations are performed on the dimer up to octamer chains in the ground state and both p- and n-doped phases. The results obtained show that the conjugated system in p- and n-doped oligo(FPT)s has a higher distance with more planar chains with respect to their neutral forms. The band gap energy between the frontier molecular orbitals decreases dramatically for both ionic states, and approaches a low limiting value with increasing oligomer length. The charge delocalization through the monomer rings along the backbone oligo(FPT)s reveals that the p- and n-doped states had more suitable properties, reflecting the electron and hole transport characteristics for conductivity, respectively. The calculated first excitation energies for oligo(FPT)s at the time-dependent B3LYP/6-31G(*d*,*p*) level of theory indicate that both doped oligomers have lower excitation energies, which display a red shift in their absorption spectra. For polymeric systems, the evolution of ionization potential, electron affinity, electron chemical potential, molecular hardness, and thermodynamic stability is made through the extrapolated oligomer ones.

DOI: 10.1134/S0022476618060069

Keywords: conducting polymer, oligo(*p*-fluorophenylthiophene), density functional theory, doped state.

INTRODUCTION

Great interest has recently been aroused in π-conjugated organic materials due to their potential applications in electronic devices, electrochromic displays, batteries, and a number of electrode-active materials in electrochemical capacitors [1-10]. These applications are achievable due to their effective conjugated length and the degree of electronic delocalization present in the polymer backbone. Conjugated polymers tend to be in the oxidized (p-doped) or reduced (n-doped) state, in which the polymer backbone is charged and has a high electronic conductivity. The reduction of the p-doped polymer generates the ′undoped′ state which is usually insulating or semi-insulating.

Faculty of Chemistry, Shahrood University of Technology, Shahrood, Iran; hnikoofard@shahroodut.ac.ir. The text was submitted by the authors in English. *Zhurnal Strukturnoi Khimii*, Vol. 59, No. 6, pp. 1338-1347, July-August, 2018. Original article submitted July 9, 2017.

***** Supplementary materials are available for this article at doi 10.1134/S0022476618060069 and are accessible for authorized users.

Along with a limited number of conducting polymers, those constructed of thiophene (T) derivatives can exist in both oxidized (p-doped) and reduced (n-doped) phases [11-13]. The polymers that can be both p- and n-doped electrochemically are attractive for the use in energy-storage devices [14, 15] and organic light-emitting diodes (OLEDs) [16-18]. A combination of an n-doped and p-doped polymers in an appropriate electrolyte solution can be utilized in a charge-storage device. Sato and co-workers have found that poly(phenylthiophene) can be applied to a *p*-*n* junction diode [13, 19]. Also, it has been found that the charge capacity and reversibility associated with n-doping of polythiophene are not as good for p-doping [20]. In this regard, Roncali and co-workers [21-23] have demonstrated that n-doping densities of polythiophenes can be increased by derivatization with phenyl or a fluorine-substituted phenyl group at position 3 of thiophene attached via different linkages.

Poly-3-(*p*-fluorophenyl)-thiophene (PFPT) is an interesting class of materials for the use in electrochemical capacitors owing to the combination of a high capacitive energy density and a low material cost. PFPT exhibits reversible p- and n-doping to a high charge density in comparison with poly(phenylthiophene). In the case of *n*-dopable conducting polymers, this is a significant improvement over that obtained previously [24-26], and this explains why PFPT could be a suitable electrode material for an electrochemical capacitor, whereas the other *p*- and *n*-dopable conducting polymers are not. Rudge *et al*. [27] have reported that high power densities can be obtained in electrochemical capacitors based on PFPT, which is very close to the current goal of the US Department of Energy for the volumetric energy density in an electrochemical capacitor for electric vehicle applications.

In a recent publication [28], we have reported the DFT/hybrid functional calculations studying a number of monomers based on phenylthiophenes (PTs) substituted with various fluorine atoms at the *ortho*-, *meta*-, and *para*-positions of the phenyl ring. It was established that delocalization of the π-conjugated system for n-doping could be highly improved for PTs functionalized with fluorine atoms. We demonstrated that the specific features of fluorinated monomers were related to the steric and electronic effects of substituents through the consideration of a number and position of fluorine atoms on the phenyl ring. An improvement over the 3-(*p*-fluorophenyl)-thiophene (FPT) was found as compared to other fluorinated PTs. The purpose of the current work was to investigate the planarity, electronic structure, conjugated length, and spectral and energetic properties of a series of oligomers made up of a FPT monomer (*n*FPT; with $n = 2$-8 repeating units) in the reduced and oxidized states. For the shorter neutral oligomers, *n*FPT with $n = 2$, the optimized molecular structure is illustrated in Scheme 1. The results obtained may be used for a desirable design of novel functional materials for conducting polymers with a high redox activity in both reduced and oxidized phases with respect to the reference thiophene (T) system.

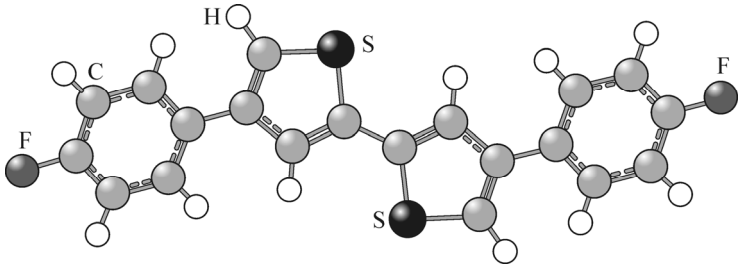

Scheme 1. Optimized molecular structure for a dimer chain of *n*FPT (with $n = 2$).

COMPUTATIONAL DETAILS

Molecular structures of the FPT oligomers up to octamer were fully optimized using the gradient procedure in DFT, as implemented in the Gaussian 09 program package [29]. DFT approaches are now the preferred method for the electronic structure theory for the π-conjugated systems and organometallic compounds [30-33]. A preliminary basis set test performed

for the calculations carried out on the electronic ground state of the short oligomer chains showed that 6-31G(*d*,*p*) was the best basis set that could be used within our available hardware/software facilities in a reasonable period of time. The optimized structures were confirmed to be the real minima through the construction and diagonalization of the corresponding Hessian matrices. The ionization potential (IP) and electron affinity (EA) values were determined as the electron energy difference between the neutral and radical cation and radical anion species, respectively. All radical cation and radical anion species were treated as open shell systems at the UB3LYP/6-31G(*d*,*p*) level of theory. The electronic chemical potential (μ) and molecular hardness (η) values were also calculated using the Koopmans theorem eigenvalues; the calculations and detailed descriptions have been reported in the literature [34, 35]. For all FPT oligomers, the standard molar enthalpies of formation in the gas phase at 298.15 K were calculated by the atomization energy route. A detailed description of the calculation procedure has been reported in the literature [41]. The time-dependent density functional theory (TD–DFT) technique was employed to calculate the ten lowest excitation states of each species.

RESULTS AND DISCUSSION

Optimized molecular structures. Since the electronic and optical properties of conducting polymers are dependent on their structural features, it is highly desirable to optimize the molecular structures of the *n*FPT and *n*T species in the ground state and their radical anion and radical cation forms. It is known that the carbon atoms adjacent to the heteroatom in the thiophene ring (α-positions) are branching centers in the electro-polymerization process, and thus, control the stereochemistry of the polymer chains. It has been found that the well-defined polymer structure contains almost exclusively the head-to-tail (H–T) conformation due to α–α couplings between the adjacent monomer rings in the backbone of the polymer chains [36, 37]. Also considering the fact that oligothiophene has a flat structure in the crystalline phase [38], the H–T conformation in which two adjacent thiophene rings are coplanar was chosen as the initial structure for the geometry optimization of FPTs at the B3LYP/6-31G(*d*,*p*) level of theory. One of the important structural parameters related to the extent of π-electron conjugation of the polymer is the chain planarity, which can be reflected by the torsion angle between the two adjacent building units along the oligomer chain (θ = ∠S–C–C–S). The θ values calculated at the B3LYP/6-31G(*d*,*p*) level of theory for all the studied species and their corresponding ionic states (doped forms) are given in Table S1 (Table S1) in the Supporting Information section. The results obtained indicated that the structure of each reference system (*n*T) had a completely planar structure (θ = 180°), in which the *n*FPT oligomers were away from the structure planarity due to the steric hindrance of the fluoro-substituted phenyl groups. In all FPTs, these departures reduced considerably in the doping process of the neutral oligomers (semi-insulating form) into the p- and n-doped oligomers (conductive forms). For an octamer chain (*n* = 8) of FPT and both its p- and n-doped states, the calculated value for |θ| along the oligomer chain was tabulated in Table 1. According to this table, our calculations indicated that the repeating units in the backbone of octa-FPT were twisted from the structure planarity ($23 < |\theta| < 40°$) due to their steric hindrance but the reduction and oxidation processes, corresponding to n- and p-doping, respectively, caused a lower value in their torsion angles ($1 < |\theta| < 23°$). This may be

TABLE 1. Average Interring Dihedral Angles |θ|, Along an Octa-FPT Chain in the Ground and Both Doped States

n	Ground state	n-doped	p-doped
2	23	2	2
3	33	12	12
4	35	14	13
5	37	17	10
6	39	19	10
7	39	20	11
8	40	23	14

attributed to the higher conjugated length in the doped oligomers. It is interesting that all the p-doped oligomers have a higher planarity with respect to the corresponding n-doped ones (about 10° for long chain $n > 4$ units). It is known that the planarity of the conducting polymer chains plays an important role in their redox activity. This result is in agreement with the experimental ones obtained by Roncali *et al*. [21-23]. The calculated results also showed no significant increase in the interring torsion angle along the oligomer chain with an increase in the repeating units.

In order to investigate the effect of the fluorophenyl substituent on the π-conjugation system, some C–C and C=C bond lengths along the conjugated backbone of the *n*FPT and *n*T species were tabulated in Table S2 (Table S2 of Supplementary Materials). In this way, the average bond alternation parameter ($\overline{\delta}$) was defined as the mean value of difference between two adjacent single C–C and double C=C bonds (displayed in Table 2, column 2). According to this table, the average bond alternation parameter for *n*FPTs decreases with increasing oligomer chain length. A suitable π-conjugation system corresponds to a lower δ value. The doping process could lead to a decrease in the $\overline{\delta}$ value. For octa-FPT in the ground and both its doped states, the $\overline{\delta}$ values varied in the following order: neutral (0.056 Å) > n-doped (0.028 Å) > p-doped (0.026 Å). In other words, the oligomers in the conductive forms, especially the p-type one, show a better π-conjugation system as compared to the neutral states.

Another structural parameter related to the π-conjugation system is the quinoid coefficient f_n [39-41]. This quantity refers to a structure in which the interring bond has a greater double bond character than that in the standard aromatic configuration, and is defined as

$$f_n = \frac{\overline{R}_{\text{Single}}}{\overline{R}_{\text{Double}}}, \tag{1}$$

where $\overline{R}_{\text{Single}}$ and $\overline{R}_{\text{Double}}$ are the mean lengths of the single C–C and double C=C bonds along the π-conjugated system, respectively. The calculated values for the quinoid coefficients of all the studied oligomers are listed in Table 2 (column 3). It was found that an f_n quantity closer to unity corresponded to an enhancement of the aromatic character of carbon bonds along the π-conjugated polymer backbone. According to Table 2, the quinoid coefficient decreases for *n*FPTs with an increase in the repeating units in the oligomer. The results obtained showed that the f_n value for the doped species was closer to unity with increasing oligomer chain length. In the case of doped octa-FPT in the ground and both its doped states, the f_8 value was closer to unity in the following order: neutral (1.042) > n-doped (1.020) > p-doped (1.018). Similar results were observed for other oligomers with different sizes. It is interesting that the quinoid coefficients for the p-doped species were lower with respect to the n-doped ones. It was also evident that the calculated results for the f_n coefficient were consistent with the behavior of the average bond alternation parameters for the FPT oligomers, as expected. The results obtained lead to satisfactory resonance structures and the improved stabilization of the conducting polymers due to the delocalization of π-electrons over the polymer backbone. Furthermore, the dependence on the oligomer chain length of the end-to-end conjugated distance ($d_{\text{end-end}}$) can be seen in Table 2 (column 4). According to this data, the end-to-end C–C conjugated

TABLE 2. Geometry Parameters, Including the Average Bond Alternation Parameter ($\overline{\delta}$), Quinoid Coefficient (f_n), and End-to-End Conjugated Distance ($d_{\text{end-end}}$) for *n*FPT (and *n*T) Oligomers

n	$\overline{\delta}$, Å	f_n	$d_{\text{end-end}}$, Å
2	0.064	1.047	8.44 (8.42)
3	0.062	1.045	14.09 (14.04)
4	0.061	1.044	19.74 (19.66)
5	0.060	1.043	25.39 (25.28)
6	0.059	1.042	31.04 (30.89)
7	0.059	1.042	36.68 (36.51)
8	0.058	1.041	42.33 (42.12)

distance as a function of the oligomer chain increased linearly. Although this distance is longer for each *n*FPT oligomer with respect to that in the corresponding reference system *n*T, it facilitates the delocalization of π electrons over the conjugated length of fluorinated PTs.

Electronic properties. The calculated Mulliken charge distributions per thiophene ring (R_i) along the oligomer chain for all the studied species are given in Table S3 (Table S3 of Supplementary Materials). In the case of octa-FTP, the charge density on R_i in the neutral and both ionic states is depicted in Fig. 1. As can be seen in this figure, a uniform charge density distribution was obtained for the doped and undoped 8FPT species. This leads to a better delocalization of the charge carrier in the oligomeric chain, and improves the conductivity [42, 43]. In neutral 8FPT, a less negative charge was distributed over the thiophene rings in the oligomer backbone. This indicates that electrons are slightly transferred from the fluorophenyl groups to the π-conjugated oligomer backbone. However, in the n/p-doped state, the main influence of the injection of one electron/hole charge is manifested in a very slight negative/positive increase in the charge on the central thiophene rings. One can expect an improvement in the charge transition along the conjugated system. A similar trend was also observed for different sizes of *n*FPTs.

It is found that the uniform distribution of the spin density in the π-conjugated system results in a better delocalization of a charge carrier in the oligomeric chain, and it improves the conductivity. In the case of the radical cation state, the diagrams for the spin density distribution on the carbon atoms along the conjugated 4FPT, 6FPT, and 8FPT chains were drawn in Fig. 2. The results obtained show that the spin density is symmetrically divided on the carbon atoms of the conjugated chains, and an increase in the oligomer chain length causes a more uniform distribution of the spin density along the oligomer backbone. A similar trend was also found for each radical anion species. Hence, the delocalization of unpaired spins on the oligomer chains leads to satisfactory resonance structures, which reflects an improvement in the charge transfer of the p- and n-doped oligomers. The results obtained are in line with those obtained by the charge distribution calculations.

For the case of *n*FPT, the delocalization of π-electrons on their molecular structure may lead to satisfactory resonance systems and improved stabilizations. The extended aromatic structure may correspond to a narrow gap between the highest occupied molecular orbital and the lowest unoccupied molecular orbital (HOMO and LUMO, respectively) which provides a reasonable qualitative indication of the excitation properties and the possibility of electron or hole transport [44, 45]. For the *n*FPT and *n*T derivatives, the HOMO and LUMO energies calculated at the B3LYP/6-31G(*d*,*p*) level of theory are given in Table S4 (Table S4 of Supplementary Materials). It was found that the closing of position 3 in the thiophene rings by fluorophenyl groups destabilized both HOMO and LUMO energy levels. In Fig. 3, for the case of nFPTs in the neutral and both doped states, the values of the HOMO–LUMO gaps (H–L gaps) are plotted against the inverse chain length (n^{-1}). It is worth noting that the H–L gaps for all FPTs decrease with increasing chain length. A similar tendency was also found for both doped states. According to Fig. 3, a reduction in the H–L gap values for both doped states becomes more

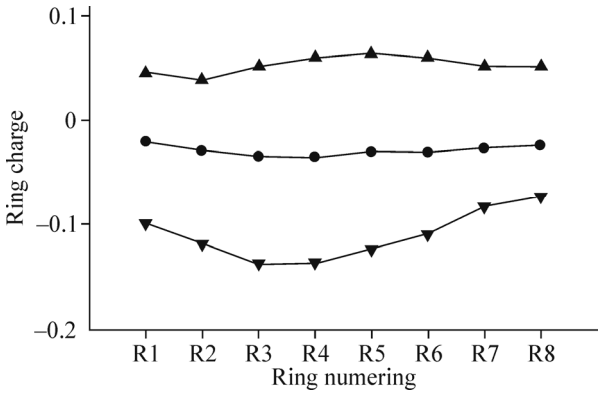

Fig. 1. Charge distribution on thiophene rings along octa-FPT for neutral (circle), radical cation (up traingle), and radical anion (down triangle) states.

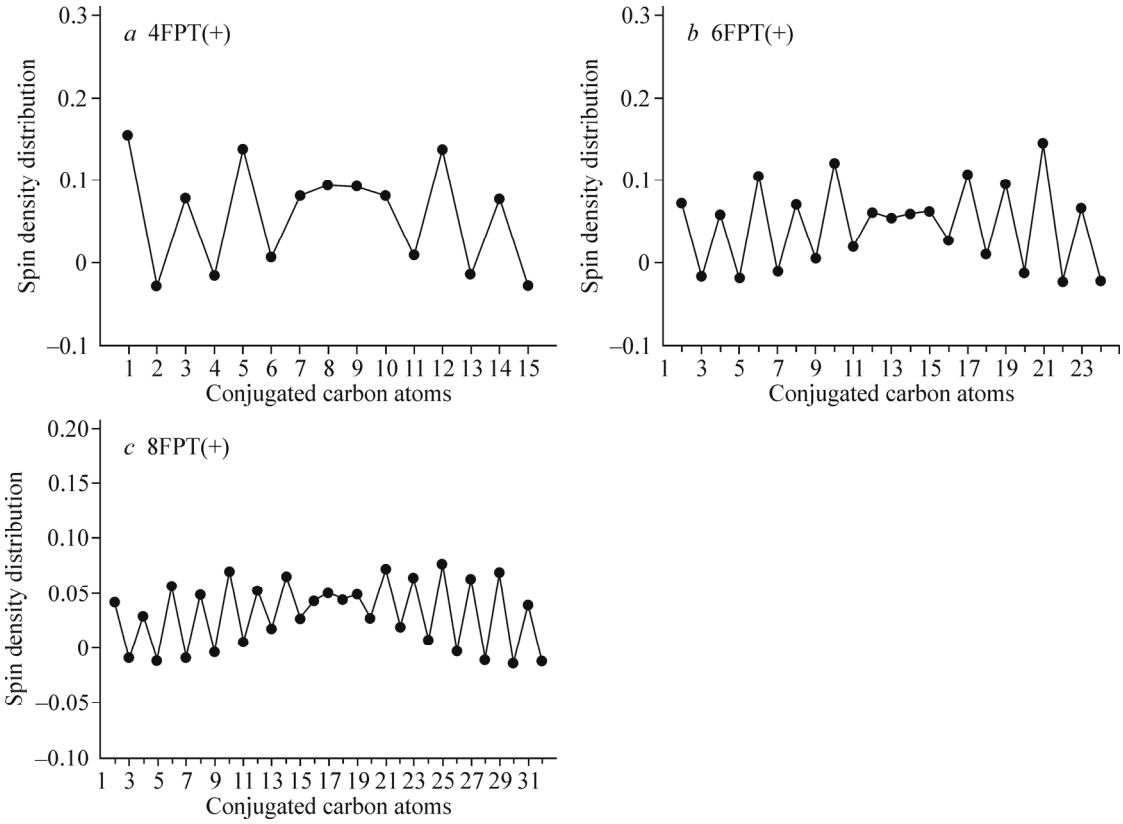

Fig. 2. Spin density distribution over the conjugated carbon atoms of 4FPT(+) (*a*), 6FPT(+) (*b*), and 8FPT(+) (*c*) radical cation oligomers.

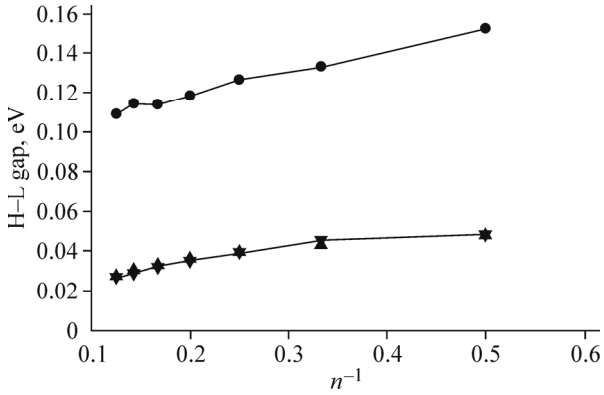

Fig. 3. Plot of H–L gap values *vs.* the inverse oligomer chain for *n*FPTs at neutral (circle), radical cation (triangle up), and radical anion (triangle down) states.

considerable with respect to their neutral states (on average, 30%), whereas this reduction is the same for each of them. By means of Fig. 3, the extrapolated H–L gap for poly(FPT) was found to be 0.02 eV.

It is well-known that the ionization potential (IP) and the electron affinity (EA) are two important parameters used for estimating the energy barrier for the injection of holes and electrons into the polymer backbone, respectively. Theoretical data obtained for an efficient hole injection to form the p-type oligomers and an efficient electron injection to form the n-type ones can be used for a rational design of a conducting material with the desired electronic and optical properties. For the case of *n*FPTs and the *n*T reference system, the IP and EA values were plotted against the inverse chain length in Fig. 4. As can be seen in Fig. 4*a*, as the oligomer chain length increases, both *n*FPT and *n*T oligomers show a lower positive IP value

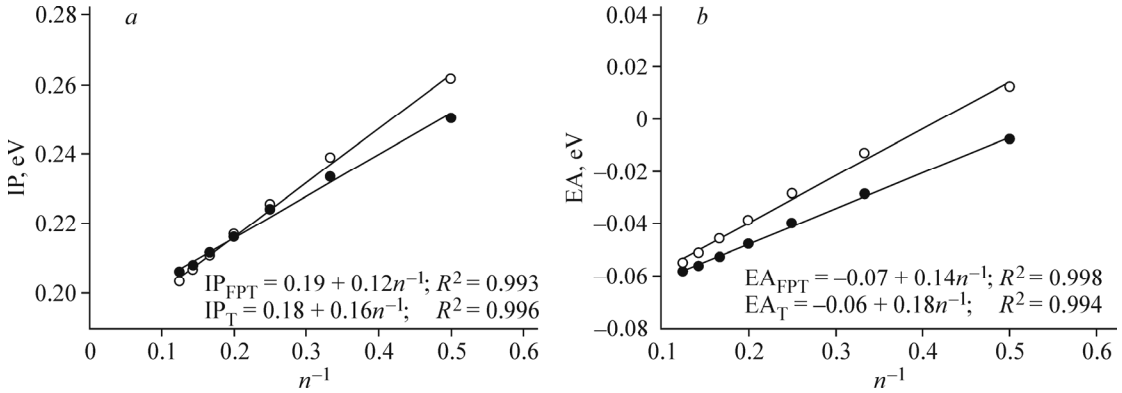

Fig. 4. Plots of IP (*a*) and EA (*b*) *vs.* the inverse oligomer chain for *n*FPT (black circle) and *n*T (white circle) oligomers.

corresponding to a less energy barrier for the hole injection. A small IP value for the *n*FPT oligomers related to a high level of the electron density delocalization in aromatic systems is due to the fluorophenyl substitution effect. Also, according to Fig. 4*b*, as the oligomer chain length increases, both oligomer types show a higher negative value for EA corresponding to the electron capture facility. Hence, the escaping tendency of electrons in the structures of FPT oligomers is stabilized by the electron-withdrawing character of the fluoro substituent. The observed behavior corresponds to an improvement in the charge carrier injection properties, which is in agreement with increasing electron conjugation of the molecules. Although our calculated oligomer data are underestimated, extrapolated theoretical IP (0.19 eV) and EA (–0.07) for poly(FPT) can be used to predict the redox potential. In fact, our calculation results were obtained for isolated molecules in the gas phase, which were different from experiment in the electrolyte solution phase. In the same way, the extrapolated IP and EA values for poly(T) were found to be 0.18 eV and –0.06 eV, respectively. In other words, the IP value for poly(FPT) was shifted to more positive values and its EA value is more negative when a fluorophenyl substituent was placed on the thiophene ring. This trend is in agreement with the oxidation and reduction rates (corresponding to the anodic and cathodic currents) for the ground state neutral poly(FPT) obtained from the cyclic voltammetry experiments [27]. It was found that the p- and n-doping of poly(FPT) were better in term of achievable charge density than poly(PT) and poly(T) [27]. It is expected that a higher electron-withdrawing character of the fluorine substituent destabilizes the product of the electro-oxidation reaction.

In the conceptual DFT perspective, the electronic chemical potential (μ) and molecular hardness (η) are the global properties that characterize the electron injection and charge transport of the molecular system [34, 35]. The electronic chemical potential is associated with the escaping tendency of electrons from the equilibrium system, and the molecular hardness is related to the resistance to charge transfer. Fig. 5*a*, *b* show the μ and η values, respectively, plotted *vs*. the inverse chain length of the oligomers. According to this figure, the plot of μ and η values correlated quite well with the oligomer size

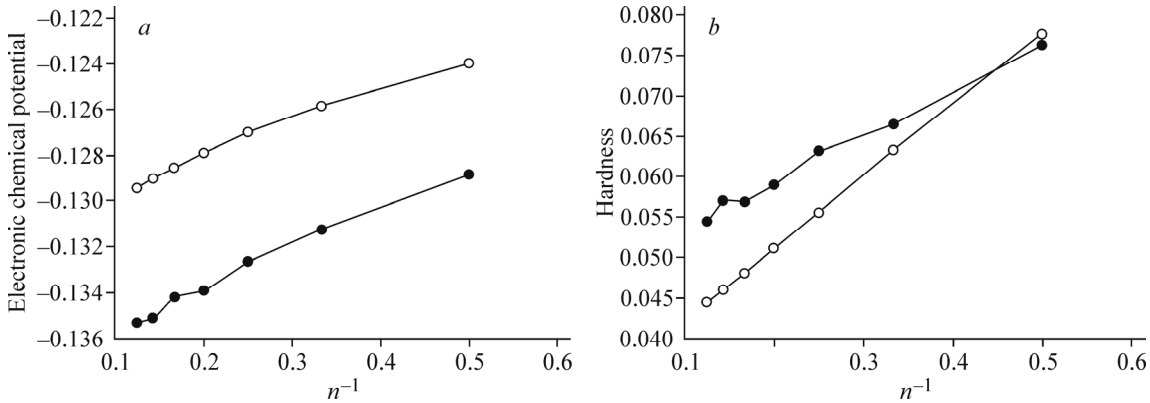

Fig. 5. Plots of electronic chemical potential (*a*) and molecular hardness (*b*) *vs.* the inverse oligomer chain for *n*FPT (black circle) and *n*T (white circle) oligomers (in eV).

for both *n*FPT and *n*T species. The μ values for the *n*FPT oligomers are larger (in the negative sign) than those for the reference oligomer *n*T. The results obtained indicate that the escaping tendency of electrons in the *n*FPT oligomers is stabilized by the electron-withdrawing character of the fluorophenyl substituent. In a similar way, according to Fig. 5*b*, the smaller η value for the *n*FPT oligomers corresponds to a higher reactivity with respect to the reference oligomer. It can be decided that the fluorophenyl substituent has a significant effect on the improvement of the charge transport via a reduction in the HOMO–LUMO gap energy. Rudge *et al*. [27] have further demonstrated that the anodic and cathodic peak currents of poly(FPT) related to the oxidation and reduction rate of the polymer, respectively, increase remarkably with respect to the unsubstituted polymer under the same experimental conditions.

Thermodynamic stability. Table S5 displays the absolute thermochemical parameters of the studied oligomers, including zero-point energy (ZPE), total energy (*E*), enthalpy (*H*), and Gibbs free energy (*G*), calculated at 298.15 K at the B3LYP/6-31G(*d*,*p*) level of theory. For a series of *n*FPT oligomers, the gas phase standard molar enthalpies of formation at 298.15 K, $\Delta H^0_{f,298}(g)$ were calculated through the atomization energy route [46] and plotted *vs*. the inverse chain length in Fig. 6. The results obtained show that the attachment of a fluorinated phenyl group to a thiophene ring leads to an evident reduction in the $\Delta H^0_{f,298}(g)$ value for the *n*FPT oligomers. According to Fig. 6, the thermodynamic stabilization of oligo(FPT)s increases non-linearly with increasing oligomer chain. Occasionally, the extrapolated $\Delta H^0_{f,298}(g)$ value (*ca.* 100 kcal/mol) can be used to predict the thermodynamic stability of poly(FPT), for which the respective experimental determination has not been reported.

UV-Visible spectral characteristics. The theoretically simulated UV-Visible spectra, including the TD–DFT excitation energies (E_g) and longest wavelengths (λ_{max}) for the maximum absorption peaks together with the corresponding oscillator strengths (*f*) of each nFPT and the reference system of oligomers are given in Table S6 (Table S6 of Supplementary Materials). The understanding of the relationship between the low-lying excited states of the π-conjugated system and their charge transport properties is a key point in providing good candidates for the design of conducting polymers. The study of the excited states by the TD–DFT [47, 48] technique is an important tool to qualitatively elucidate the mechanism of the electron and hole transfer in the *n*FPT oligomers. For a series of *n*FPT oligomers from the dimer up to the hexamer in the ground and both doped states, the values for the simulated absorption spectral properties were compared, and the results obtained were tabulated in Table 3.

As can be seen in this table, by increasing the oligomer chain length, an evident bathochromic shift and thus a decrease in the E_g values were obtained. In comparison with the ground state of *n*FPT derivatives, the n- and p-doped states have larger λ_{max} values, owing to their higher conjugated lengths and planarity. The observed trend in the simulated absorption spectral properties (Table 3) is similar to that obtained for the HOMO–LUMO gap energies. It could be concluded

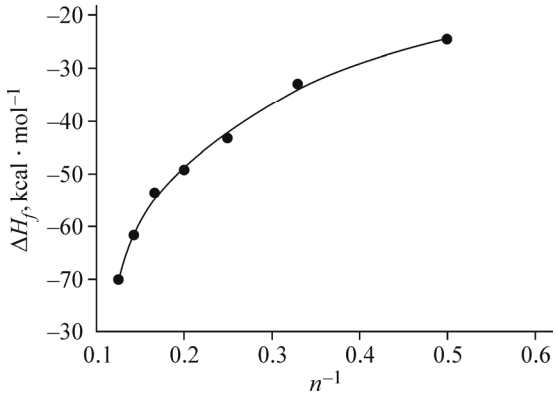

Fig. 6. Plot of gas-phase standard molar enthalpies of formation at 298.15 K for *n*FPT oligomers *vs.* the inverse oligomer chain.

TABLE 3. E_g (eV) and λ_{max} (nm) Values for the Simulated Absorption Spectra of oligo(FPT)s in the Ground and Both Doped States at the TD-B3LYP/6-31G(*d*,*p*) Level of Theory

n	Ground state		n-doped		p-doped		*n*	Ground state		n-doped		p-doped	
	E_g	λ_{max}	E_g	λ_{max}	E_g	λ_{max}		E_g	λ_{max}	E_g	λ_{max}	E_g	λ_{max}
2	3.36	321	0.49	2540	0.71	1739	6	2.07	599	0.78	1585	0.75	1653
3	3.29	377	0.66	1888	0.71	1737	7	1.97	628	0.69	1804	0.67	1857
4	3.02	410	0.72	1728	0.66	1893	8	1.88	660	0.62	1989	0.67	1863
5	2.21	562	0.88	1408	0.81	1522							

that poly(FPT) is a good candidate for the ambipolar charge transfer semi-conductors in charge-storage applications. Furthermore, the simulated excitation spectra obtained using a Gaussian broadening for the six lowest excitation states of di-, tetra-, hexa-, and octa-FPTs were demonstrated in Fig. 7. The peak concerned with the π–π* transition showed a bathochromic shift toward the higher wavelengths of 321 nm, 410 nm, 599 nm, and 660 nm, related to 2, 4, 6, and 8 repeating units, which is due to an increase in the extent of the conjugated length. Finally, it is concluded that the fluorine substitution can modify some of the physical and electronic characteristics of poly(FPT). This effect can be related to the steric and electronic effects of the F substitution through the contribution of fluorophenyl ring on the delocalization of the π electron density in aromatic systems.

CONCLUSIONS

The DFT-B3LYP/6-31G(*d*,*p*) level of theory was used for the *n*FPT oligomers, where $n = 2$-8 repeating units, in order to study the effect of the *para*-fluorophenyl substituent on the geometry, electron conjugation, and spectral and energetic properties of poly(FPT). In comparison with the reference *n*T system, it was found that the *n*FPT oligomers were twisted from the structure planarity (less than 40°) due to the steric strain of the fluorophenyl substituent attached to the thiophene rings of the conjugated system. This departure reduced significantly in the reduction/oxidation phase, in which the n/p-doped polymer had more satisfactory features for the conductivity. The results obtained showed that the hole injection to form the p-type conductive polymers was more favorable than the electron injection to form the n-type ones. A number of electronic properties such as the H–L gap, IP, EA, μ, and η correlated linearly with the inverse oligomer length and their extrapolated

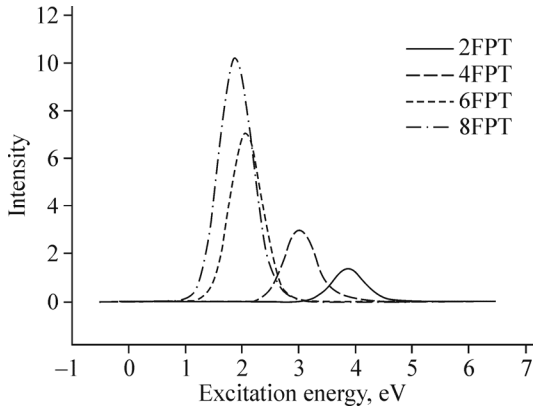

Fig. 7. Simulated absorption spectra for dimer (solid line), tetramer (long-dash line), hexamer (short-dash line), and octamer (dash-dot-line) FPT oligomers calculated at the TD-B3LYP/6-31G(*d*,*p*) level of theory (relative oscillator strengths are given in arbitrary units).

values might be used for poly(FPT). The simulated UV-Visible absorption spectral analysis showed that both n- and p-doped oligomers had lower excitation energies in comparison with the ground state, which is in good agreement with the results obtained for the H–L gap investigations. In addition, our calculated results for the standard molar enthalpies of formation showed that the thermodynamic stabilization of oligo(FPT) increased non-linearly with an increase in the oligomer chain, indicating a good electron delocalization over the polymer backbone. The stabilization energy value for poly(FPT) was estimated to be 100 kcal/mol.

The financial support of Shahrood University of Technology is gratefully acknowledged.

REFERENCES

1. S. S. Sun and N. S. Sariciftci. Organic Photovoltaics, Mechanisms, Materials and Devices. New York: CRC Press, **2005**.
2. H. He, J. Zhu, N. J. Tau, L. A. Nagahara, I. Amlani, and R. Tsui. *J. Am. Chem. Soc.*, **2001**, *123*, 7730.
3. Z. H. Kafafi. Organic Electroluminescence. Taylor and Francis, New York, **2005**.
4. J. M. Yeh, C. L. Chen, C. Y. Ma, K. R. Lee, Y. Wei, and S. Li. *Polymer*, **2002**, *43*, 2729.
5. C. D. Entwistle and T. B. Marder. *Chem. Mater*., **2004**, *16*, 4574.
6. Y. Sun and S. Wang. *Inorg. Chem*., **2010**, *49*, 4394.
7. X. Lin, J. Li, E. Smela, and S. Tip. *Int. J. Quantum Chem*., **2005**, *102*, 980.
8. G. Garcia, A. Garzon, J. M. Granadino-Roldan, M. Moral, A. Navarro, and M. Fernandez-Gomez. *J. Phys. Chem. C*, **2011**, *115*, 6922.
9. M. Mushrush, A. Facchetti, M. Lefenfeld, H. E. Katz, and T. J. Marks. *J. Am. Chem. Soc*., **2003**, *125*, 9414.
10. H. Spanggaard and F. C. Krebs. *Sol. Energy Mater. Sol. Cells*, **2004**, *83*, 125.
11. K. Kaeriyama, S. Tanaka, M. A. Sato, and K. Hamada. *Synth. Met*., **1989**, *28*, 611.
12. K. Kaneto, S. Ura, K. Yoshino, and Y. Inuishi. *Jpn. J. Appl. Phys*., **1984**, *23*, L189.
13. M. A. Sato, S. Tanaka, and K. Kaeriyama. *J. Chem. Soc.*, *Chem. Commun*., **1987**, 1725.
14. R. M. Crooks, O. M. R. Chyan, and M. S. Wrighton. *Chem. Mater*., **1989**, *1*, 2.
15. J. P. Ferraris and T. L. Lambert. *J. Chem. Soc.*, *Chem. Commun*., **1991**, 1268.
16. A. C. Grimsdale, K. L. Chan, R. E. Martin, P. G. Jokisz, and A. B. Holmes. *Chem. Rev*., **2009**, *109*, 897.
17. P. Heremans, D. Cheyns, and B. P. Rand. *Acc. Chem. Res*., **2009**, *42*, 1740.
18. S. Gűnes, H. Neugebauer, and N. S. Sariciftci. *Chem. Rev.*, **2007**, *107*, 1324.
19. M. A. Sato, S. Tanaka, and K. Kaeriyama. *Makromol. Chem*., **1989**, *190*, 1233.
20. J. Roncali. *Chem. Rev*., **1992**, *92*, 711.
21. J. Roncali, H. K. Youssoufi, R. Garreau, F. Garnie, and M. Lemaire. *J. Chem. Soc.*, *Chem. Commun*., **1990**, 414.
22. M. Lemaire, R. Garreau, D. Delabouglise, J. Roncali, H. K. Youssoufi, and F. Garnier. *New J. Chem*., **1990**, *14*, 359.
23. H. K. Youssoufi, R. Garreau, F. Garnier, and M. Lemaire. *J. Roncali*, *Synth. Met*., **1991**, *43*, 2916.
24. D. Ofer, R. M. Crooks, and M. S. Wrighton. *J. Am. Chem. Soc*., **1990**, *112*, 7869.
25. T. R. Jow and L. W. Shacklette. *J. Electrochem. Soc*., **1988**, *135*, 541.
26. P. A. DePra, J. G. Gaudiello, and T. J. Marks. *Macromolecules*, **1988**, *21*, 2295.
27. A. Rudge, J. Davey, I. Raistrick, S. Gottesfeld, and J. P. Ferraris. *J. Power Sources*, **1994**, *47*, 89.
28. H. Nikoofard. *J. Fluorine Chem*., **2016**, *185*, 181.
29. M. J. Frisch, G. W. Trucks, H. B. Schlegel, G. E. Scuseria, M. A. Robb, J. R. Cheeseman, V. G. Zakrzewski, J. A. Montgomery Jr., R. E. Stratmann, J. C. Burant, S. Dapprich, J. M. Millam, A. D. Daniels, K. N. Kudin, M. C. Strain, O. Farkas, J. Tomasi, V. Barone, M. Cossi, R. Cammi, B. Mennucci, C. Pomelli, C. Adamo, S. Clifford, J. Ochterski, G. A. Petersson, P. Y. Ayala, Q. Cui, K. Morokuma, D. K. Malick, A. D. Rabuck, K. Raghavachari, J. B. Foresman, J. Cioslowski, J. V. Ortiz, B. B. Stefanov, G. Liu, A. Liashenko, P. Piskorz, I. Komaromi, R. Gomperts,

R. L. Martin, D. J. Fox, T. Keith, M. A. Al-Laham, C. Y. Peng, A. Nanayakkara, C. Gonzalez, M. Challacombe, P. M. W. Gill, B. Johnson, W. Chen, M. W. Wong, J. L. Andres, C. Gonzalez, M. Head-Gordon, E. S. Replogle, and J. A. Pople. Gaussian 09W, Gaussian Inc., Pittsburgh PA, **2009**.
30. G. L. Zhang, H. Zhang, D. P. Li, D. Chen, X. Y. Yu, B. Liu, and Z. S. Li. *Theor. Chem. Acc.*, **2008**, *121*, 109.
31. U. Salzner, P. G. Pickup, R. A. Poirier, and J. B. Lagowski. *J. Phys. Chem*. *A*, **1998**, *102*, 2572.
32. C. J. Cramer and D. G. Truhlar. *Phys. Chem. Chem. Phys*., **2009**, *11*, 10757.
33. S. Suramitr, A. Piriyagagoon, P. Wolschann, and S. Hannongbua. *Theor. Chem. Acc*., **2012**, *131*, 1209.
34. R. G. Parr, L. V. Szentpaly, and S. Liu. *J. Am. Chem. Soc*., **1999**, *121*, 1922.
35. J. L. Moncada and A. Toro-Labbe. *Chem. Phys. Lett*., **2006**, *429*, 161.
36. H. Sabzyan and H. Nikoofard. *Chem. Phys*., **2004**, *306*, 105.
37. H. Nikoofard and M. Gholami. *C.R. Chimie*., **2014**, *17*, 1034.
38. R. Azumi, G. Götz, T. Debaerdemaeker, and P. Bäuerle. *Chem. Eur. J*., **2000**, *6*, 735.
39. M. Levy and A. Nagy. *Phys. Rev. Lett*., **1999**, *83*, 4361.
40. A. Omrani and H. Sabzyan. *J. Phys. Chem*. *A*, **2005**, *109*, 8874.
41. R. Colle and A. Curioni. *J. Phys. Chem*. *A*, **2000**, *104*, 8546.
42. R. J. Waltman, A. F. Diaz, and J. Bargon. *J. Phys. Chem*., **1984**, *88*, 4343.
43. A. Hlel, A. Mabrouk, M. Chemek, and K. Alimi. *Spectrochim. Acta A*, **2012**, *99*, 126.
44. M. A. De Oliveira, H. Duarte, J. Pernaut, and W. B. De Almeida. *J. Phys. Chem*. *A*, **2000**, *104*, 8256.
45. H. Cao, J. Ma, G. Zhang, and Y. Jiang. *Macromolecules*, **2005**, *38*, 1123.
46. J. W. Ochterski. Gaussian white paper, Thermochemistry in Gaussian 2000; http://www.gaussian.com/g_white-pap/thermo.htm.
47. Z. H. Levine and P. Soven. *Phys. Rev. A*, **1984**, *29*, 625.
48. D. Jacquemin, E. A. Perpete, I. Ciofini, and C. Adamo. *Acc. Chem. Res*., **2009**, *42*, 326.